Development of Spin Coat Modeling Techniques

Meghann L. Dunn, Nathan Girard, Rhiannon Lecuyer, and Richmond Tetteh
Department of Physics, University of Massachusetts Boston, Boston, Massachusetts 02125, USA
(Dated: January 26, 2026)

Spin coating is a standard technique for producing uniform thin films in materials science. Although the governing physics is well understood, researchers still rely heavily on trial-and-error to determine optimal spin parameters. Commercial spin coaters do not provide theoretical predictions of the final film thickness, which wastes time and material and introduces inconsistency in film thickness. To address this, we test whether incorporating material rheological parameters into a MATLAB model can reliably output the required spin-up and spin-off angular velocity profiles. To test the model's ability to predict the spin settings required to achieve a desired final film thickness, we use material-specific rheological properties of PVK in chlorobenzene and cellulose acetate in diacetone; two widely used coating solutions. The resulting film thicknesses from experimental data are then measured and compared with the film heights predicted by the simulation. The agreement between the two validates the model's accuracy and consistency and provides a more systematic, consistent approach to thin-film fabrication.

I. INTRODUCTION

Spin coating has historically been a reliable technique in coating microscope slides with thin films in materials science. Although the method is widely used, many researchers often have to use trial and error to get the correct spin coat settings, and the material properties of the samples used in spin coating are often ignored.

Spin coaters are relatively simple devices: the user sets a desired angular velocity and a time for the material to spin at. There are four required inputs on the spin coater; two per spin cycle, each spin cycle having its own time and angular velocity. However, material properties often dictate the physics of the dispersion of the material on the slide. In current spin coating methods, the process of trial and error to find the exact settings to accurately coat a slide to the desired height can lead to much of the material having to be discarded due to inadequate film thicknesses. Assuming the sample takes ample time or money to produce, this can cost many laboratories valuable time and funding in order to find the appropriate settings.

II. MODEL

Due to standard angular velocities for most spin coating applications being low enough to simplify evaporation rate, we consider the transition point where shear thinning contributes equally to evaporation and flow [1][2]

$$E = \frac{(1 - C_0)2\omega^2 \rho h_f^3}{3\eta} \tag{1}$$

We choose this point to solve for angular velocity:

$$\omega = \left(\frac{3\eta E}{2(1 - C_0)\rho h_f^3} \right)^{1/2} \tag{2}$$

Using user inputs for the ideal height of the film, we determine the ideal transition angular velocity that the user should use as a basis for an angular velocity.

We use a standard angular velocity range of $100\,rpms$ to $8000\,rpms$ which most spin coaters implement. By solving the transition evaporation rate equation (Eq.1) and solving it for final height,

$$h_f = \left(\frac{3\eta E}{2(1 - C_0)\rho\omega^2} \right)^{1/3} \tag{3}$$

A baseline of final heights versus angular frequencies can be obtained as seen in Figure 1.

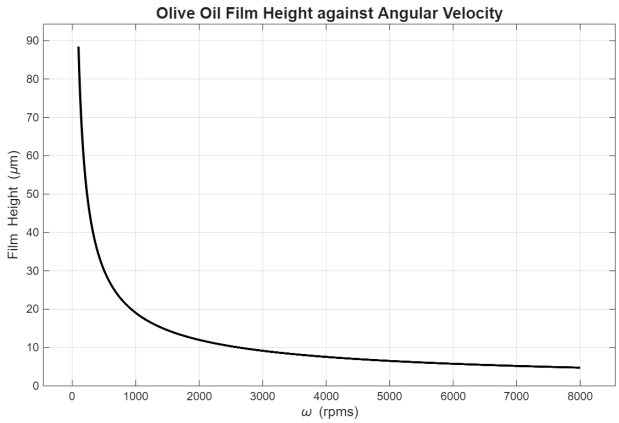

FIG. 1: *Example Output Graph for Film Height against Angular Velocity*

From here, the user can determine an appropriate angular velocity to plot height versus time. By iterating over time values and using [3][4]

$$h_f = \frac{h_0}{\left(\frac{4\rho\omega^2 h_0^2 t}{3\eta_0} + 1 \right)^{1/2}} \tag{4}$$

a final height thickness for the film can be plotted against time as seen in Figure 2. The user can implement this

feature by using the RPM override feature.

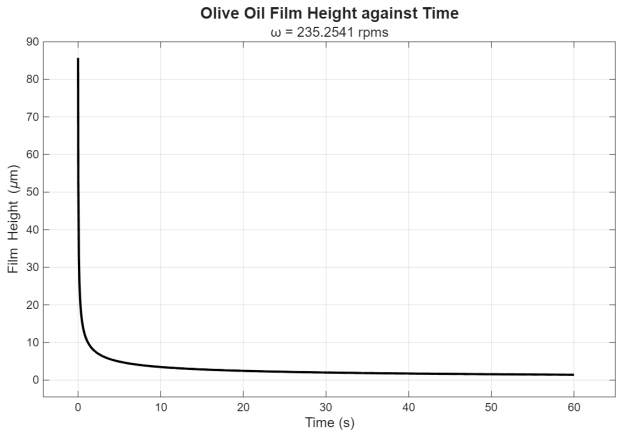

FIG. 2: *Example Output Graph for Film Height against Time*

A graphical user interface (GUI) was created to give the user easy access to the program (Figure 3) where they can input the material properties of the sample they are interested in spinning.

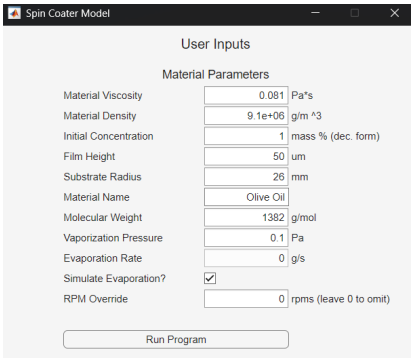

FIG. 3: *Graphical User Interface (GUI)*

With all the properties being relatively easy to experimentally obtain via a creep or flow test or by researching their accepted values.

Finally, the evaporation rate, which is arguably negligible at lower spin times [2][3][4], can be measured experimentally or simulated [5] using:

$$E = 0.058 P_{vap} \left(\frac{M_{molec}}{T} \right)^{1/2} \tag{5}$$

The model assumes shear arises mainly from radial outflow caused by centrifugal forces. The primary velocity gradient is across the film thickness, allowing reduction of the three-dimensional flow to an effective one-dimensional shear problem. This approach aligns with the lubrication approximation for thin films [3, 4]. It is also assumed that, for flat substrates and moderate angular velocities, Coriolis forces and azimuthal flow have negligible effects on film thickness evolution. These assumptions justify the use of bulk rheological parameters measured under simple shear conditions [6].

III. METHODS AND MATERIALS

The spin coating model used in this work is based on thin film hydrodynamics under centrifugal force, combined with simplified evaporation kinetics. Following standard treatments, the model assumes the film has a uniform thickness and behaves as a Newtonian fluid. The film is also considered sufficiently thin for the lubrication approximation to be valid, meaning inertial effects are negligible compared to viscous forces [2–4].

The balance between viscous flow and solvent evaporation yields the transition evaporation rate from Eq.1

$$E = \frac{(1 - C_0) 2\omega^2 \rho h_f^3}{3\eta}$$

which is adapted from classical spin coating models describing the crossover between flow-dominated and evaporation-dominated thinning regimes [1, 2, 4]. Rearranging gives the angular velocity (Eq.2) for a desired thin film and, ultimately, the final thickness h_f (Eq.3). In the viscous dominated regime, the time-dependent thinning of the film (Eq.4)

$$h_f = \frac{h_0}{\left(\frac{4\rho\omega^2 h_0^2 t}{3\eta_0} + 1 \right)^{1/2}}$$

The evaporation rate used in the model for Eq.5

$$E = 0.058 P_{vap} \left(\frac{M_{molec}}{T} \right)^{1/2}$$

is based on liquid surface evaporation and provides an estimate of solvent loss if direct measurements are unavailable [2, 5, 7].

To experimentally test our model, poly(9-vinylcarbazole) (PVK) dissolved in chlorobenzene at 2% by weight and cellulose acetate (CA) dissolved in diacetone alcohol at 2.8% by weight were used. Both solutions are organic polymer solutions and were alternately layered onto an approximately 25 mm × 25 mm cut section of a standard 75 mm × 25 mm glass microscope slide. The chosen solutions are used for the fabrication of Distributed Bragg Reflectors (DBRs), which requires alternating thin layers of two materials with contrasting refractive indices. In this system, the PVK solution provides the higher refractive index layer, while the CA solution provides the lower refractive index layer. After each spin coated layer is deposited, the substrate is baked at $110°C$ for 15 minutes to harden the film.

IV. EXPERIMENTAL RESULTS AND ANALYSIS

Rheological characterization of the coating solutions was carried out to validate the material assumptions

used in the spin coating model and to confirm that the measured parameters were physically consistent with the governing equations. Flow tests, amplitude sweeps, and frequency sweeps were performed on both PVK and CA, with additional frequency sweep measurements conducted for CA at elevated temperatures due to its thermally activated viscoelastic behavior.

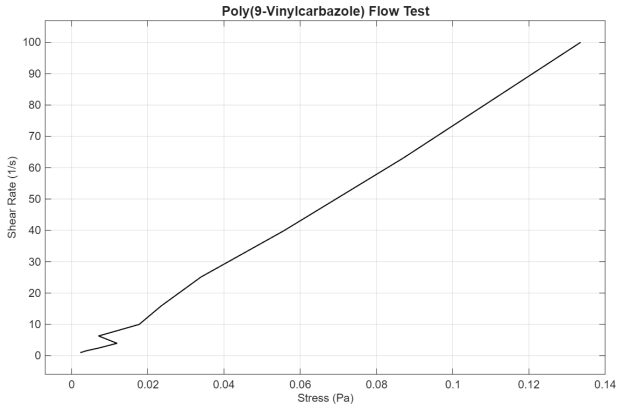

FIG. 4: *Experimental flow test data for Poly(9-Vinylcarbazole) at room temp*

Figure 4 shows the shear stress as a function of shear rate for PVK at room temperature. The data exhibited a linear relationship across the measured shear-rate range, indicating that PVK behaves like a Newtonian fluid under these conditions. This linearity implies a nearly constant viscosity, which supports the use of a single viscosity parameter in the angular-velocity and film-thickness equations employed in the spin coating model.

Similarly, Figure 5 presents the flow test results for cellulose acetate at room temperature. Despite the visually high viscosity of the solution in bulk form, the rheological data again show a linear dependence of shear stress on shear rate. This behavior suggests that, within the shear regime relevant to spin coating, the cellulose acetate solution can be reasonably approximated as a Newtonian fluid as well. This result is particularly important given that the theoretical framework assumes constant viscosity when solving for the transition angular velocity and final film thickness.

The viscoelastic properties of cellulose acetate were further examined through an amplitude sweep test, shown in Figure 6. Across the measured strain amplitudes, the loss modulus (G'') consistently exceeds the storage modulus (G'). This indicates that viscous dissipation dominates elastic energy storage, confirming a liquid-like response under small oscillatory deformations. This result is consistent with the expected behavior during spin coating, where the fluid experiences continuous shear rather than elastic deformation. The dominance of G'' supports the assumption that elastic effects are negligible during the spreading phase of the coating process and that viscous flow governs film thinning.

Additionally, combining this with Figure 5, it is apparent that there is no stress plateau at low shear rates,

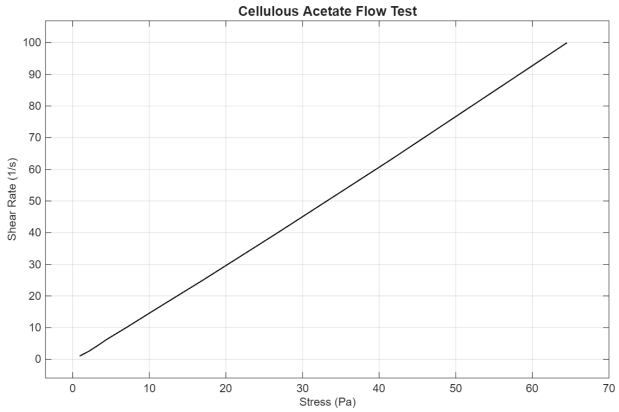

FIG. 5: *Experimental flow test data for cellulose acetate at room temp*

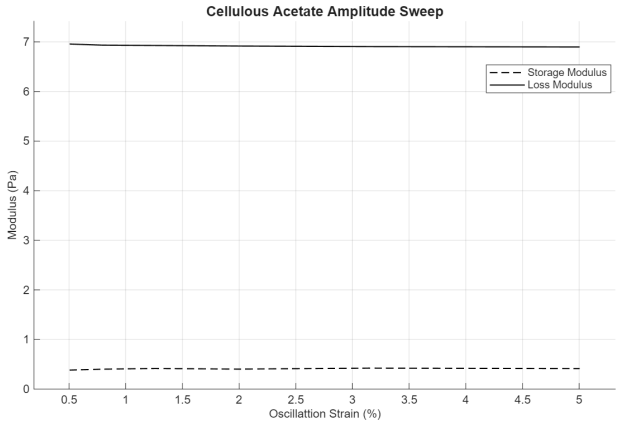

FIG. 6: *Experimental Amplitude Sweep test data for Cellulous Acetate at room temp*

indicating that CA begins to flow directly once stress is applied, meaning there is no "hold off" of the material to flow. Relating back to spin coating, once an angular velocity ω is applied, the material begins to flow instantly. Since the loss modulus is much greater than the storage modulus, as shown in Figure 6, it is further agreed that CA undergoes this "instantaneous flowing" once accelerated.

V. DISCUSSION

At the current stage of development, the model accurately predicts and plots the final film thickness as a function of rotational speed. Additionally, when an angular velocity ω is specified, the model generates the evolution of film thickness as a function of time. Several nontrivial behaviors and modeling features emerged during development; these observations are discussed below without a predefined order.

During the experiments conducted to determine material viscosity, the coating solutions were found to exhibit complex fluid behavior. In particular, the CA solution displayed strongly temperature-dependent rheology: at

room temperature it behaved as a highly viscous material, to the extent that it could not be aspirated with a pipette. Upon heating to approximately $75°C$ the solution became visually more fluid and exhibited behavior consistent with a Newtonian fluid response. However, frequency sweep measurements revealed contrasting viscoelastic behavior, as shown in Figures 7 and 8.

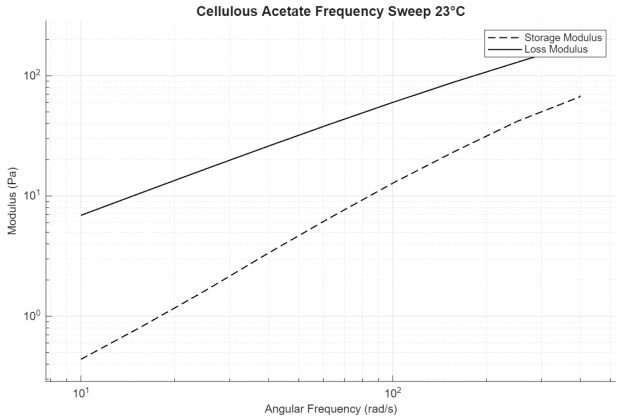

FIG. 7: *Experimental Frequency Sweep test data for Cellulous Acetate at room temp ($\sim 23°C$)*

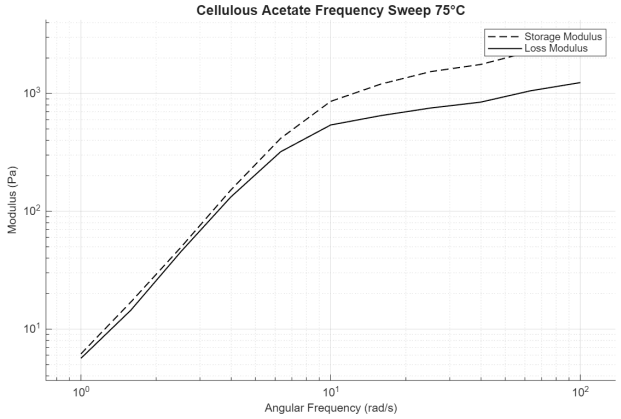

FIG. 8: *Experimental Frequency Sweep test data for Cellulous Acetate at $75°C$*

At room temperature, rheological measurements of CA indicate that $G'' > G'$ which corresponds to a more liquid-like response. This result contrasts with its physical presentation. A similar anomaly was found when the temperature of our solution is raised to $75°C$ in the rheometer: rather than exhibiting a more fluid-like response, the material became increasingly solid-like, as shown in Figure 8. One possible explanation for this behavior is the limited sample volume used in the rheological measurements. Only $600\mu L$ of each solution was dispensed for the rheological experiments, suggesting that sample volume and confinement may influence the measured response. The viscoelastic behavior observed in the frequency sweep data is consistent with the material's physical state expected after spin coating and subsequent baking. These observations further suggest that both solutions behave as Newtonian fluids only at sufficiently low concentrations.

The PVK and CA coating solutions have concentrations of 2% and 2.8%, respectively. At these dilute concentrations, polymer chains are expected to be largely non-overlapping (i.e., below the overlap concentration), so inter-chain interactions and entanglements are reduced, and the solutions may exhibit approximately Newtonian behavior. Under these conditions, the viscosity η appearing in the angular velocity relation (Eq. 2):

$$\omega = \left(\frac{3\eta E}{2(1 - C_0)\rho h_f^3} \right)^{1/2}$$

can be treated as a well-defined material parameter.

Exploration of the model revealed that the factor $(1 - C_0)$ value needs to be greater than 0.9 for the angular velocity to be realistic. Since our model applies to thin films, the h_f value is intrinsically small. Due to both $1 - C_0$ and h_f appearing in the denominator, small values of these parameters lead to a rapid increase in the predicted angular velocity ω; exceeding the physical operational limits of the spin coater. Continued development of the model would include implementing a solution to prevent nonphysical angular velocity predictions.

Overall, the experimental data validate the rheological assumptions underlying the spin coating model and demonstrate that incorporating material-specific properties provides a physically consistent and systematic approach for predicting spin coating parameters. Development of the model is ongoing.

VI. ACKNOWLEDGMENTS

We thank Dr. Jonathan Celli of the University of Massachusetts, Boston for providing a bulk rheometer to experimentally test the material properties of PVK and diacetone, Dr. Chandra Yelleswarapu of the University of Massachusetts, Boston for providing the sample materials, Dr. Mohamed Gharbi of the University of Massachusetts, Boston for providing us access to his spin coater, Dr. Olga Goulko of the University of Massachusetts, Boston for providing templates of simulation and modeling papers. Additionally, we would like to thank the New England Complex Fluids workshop for providing us the opportunity to present on this project; and the McNair Scholars program for their support, and ability to present on this project during a monthly meeting.

Portions of the text were refined with the assistance of OpenAI's ChatGPT (version GPT-5.2) and Grammarly (Grammarly, Inc., 2025). The authors take full authority of the content, interpretation, and conclusions in this report.

VII. AUTHOR CONTRIBUTIONS

Conceptualization: RL
Methodology: RL, NG
Investigation: MLD, NG, RL, RT
Visualization: NG, MD
Writing (original draft): MLD, NG, RL, RT
Writing (review, editing): MLD, NG, RL, RT

[1] J. Griffin, Spin coating: Complete guide to theory and techniques.
[2] S. Hellstrom, Basic models of spin coating, Stanford University (2007).
[3] R. Yonkoski, Model for spin coating in microelectronic applications, Journal of Applied Physics **72** (1992).
[4] M. Tyona, A theoretical study on spin coating technique, Advances in Materials Research **2** (2013).
[5] P. Danielson, Molecular flux provides process understanding, Article on Normandale Community College Vacuum and Thin Film Technology website (2001).
[6] R. G. Shepherd, A general model for spin coating on a non-axisymmetric curved substrate, Under consideration for publication in J. Fluid Mech. **A32** (2024).
[7] L. Cost Effective Equipment, Spin coat theory (2023).